

Neuropathological investigation of patients with prolonged anorexia nervosa

Ito Kawakami, MD, PhD ^{1,2*} Shuji Iritani, MD, PhD ³ Yuichi Riku, MD, PhD,^{4,5} Kentaro Umeda, MD, PhD,^{2,3} Mina Takase,¹ Kenji Ikeda, MD, PhD,¹ Kazuhiro Niizato, MD, PhD,² Tomio Arai, MD, PhD,⁶ Mari Yoshida, MD, PhD,⁴ Kenichi Oshima, MD, PhD² and Masato Hasegawa, PhD¹

Objectives: Recent neuroimaging studies have indicated that the mesolimbic pathway, known to work as reward neuronal circuitry, regulates cognitive-behavioral flexibility in prolonged anorexia nervosa (AN). Although AN is associated with the highest mortality rate among psychiatric disorders, there have been few neuropathological studies on this topic. This study aims to identify alterations of the reward circuitry regions, especially in the nucleus accumbens (NAcc), using AN brain tissues.

Methods: The neuronal networks in AN cases and controls were examined by immunohistochemistry directed at tyrosine hydroxylase (TH; dopaminergic neuron marker) and glial fibrillary acidic protein (GFAP; astrocyte marker). We also immunochemically analyzed frozen samples presenting astrogliosis, especially in the NAcc and striatum.

Results: Histologically, neuronal deformation with cytoplasmic shrinkage was seen in reward-related brain regions, such as the orbitofrontal cortex/anterior cingulate cortex. The NAcc showed massive GFAP-positive astrocytes and

dot-like protrusions of astrocytes in the shell compartment. In the shell, TH and GFAP immunoreactivities revealed prominent astrogliosis within striosomes, which receive projection from the ventral tegmental area (VTA). The numbers of GFAP-positive astrocytes in the NAcc ($P = 0.0079$) and VTA ($P = 0.0025$) of AN cases were significantly higher than those of controls. Strongly immunoreactive 18 to 25 kDa bands, which might represent degradation products, were detected only in the NAcc of AN cases. Clinically, all cases presented cognitive rigidity, which might reflect a deficit of the reward pathway.

Conclusion: Our findings suggest impaired dopaminergic innervation between the NAcc and VTA in AN. Functional dysconnectivity in the reward-related network might induce neuropsychiatric symptoms associated with AN.

Keywords: anorexia nervosa, eating disorder, neuropathology, nucleus accumbens, reward circuit.

<http://onlinelibrary.wiley.com/doi/10.1111/pcn.13340/full>

Anorexia nervosa (AN) is a serious psychosomatic eating disorder characterized by severe disturbances in eating behavior, body weight, and body/self-perception.¹ It sometimes shows familial groupings, and shared biological underpinnings have been hypothesized.² The most obvious features of AN are severe emaciation and malnourishment.³ Approximately half of the cases are chronic or recurrent, with an average medical history of more than 5 years. In patients with AN, chronic starvation can cause medical and metabolic complications affecting virtually any body system,³ and is associated with depressed mood, anxiety, obsessions, compulsions, and affective dysregulation.⁴ AN is classified into two types on the basis of eating-related behavior, ie, restricting type (loss of weight is caused purely by dieting, without binge eating or purging) and binge eating/purging type (involving restricted food intake, but also periodic disinhibition of restraint, with binge eating and/or purging).^{1,5} Transition between these syndromes frequently occurs.

The precise pathophysiology of AN remains unclear and might involve complex interactions of developmental, genetic, environmental, psychological, and neurobiological factors. Recent structural and

functional magnetic resonance imaging (fMRI) studies have focused on the role of neurocircuitry in the pathophysiology of AN, and have implicated the reward circuit that regulates food intake.^{3,5,6} The neurotransmitter dopamine modulates food reward via the mesocorticolimbic pathway of the brain, which includes the orbitofrontal cortex (OFC), anterior cingulate cortex (ACC), hippocampus, ventral striatum/nucleus accumbens (NAcc), and midbrain/ventral tegmental area.^{7,8} Those fMRI studies indicated the mesocorticolimbic pathway to be particularly vulnerable in earlier cases of AN.^{5,9,10} Dysfunction may lead to emotional processing deficits and psychiatric symptoms such as obsessive-compulsive disorder, which then drive maladaptive behaviors in AN.^{3,11}

Although AN has the highest mortality rate of any psychiatric disorder, there has been few neuropathological investigations.^{12,13} In this study, we identified five autopsy cases with prolonged AN in our archives. Considering the pathophysiological background, we planned to focus on the NAcc, which is a center of the mesocorticolimbic pathway. We evaluated the neuropathology of AN brains in comparison with control brains to identify alterations of the

¹ Dementia Research Project, Tokyo Metropolitan Institute of Medical Science, Tokyo, Japan

² Department of Psychiatry, Tokyo Metropolitan Matsuzawa Hospital, Tokyo, Japan

³ Department of Psychiatry, Nagoya University Graduate School of Medicine, Nagoya, Japan

⁴ Institute for Medical Science of Aging, Aichi Medical University, Nagakute, Japan

⁵ Department of Neurology, Nagoya University, Nagoya, Japan

⁶ Department of Pathology, Tokyo Metropolitan Geriatric Hospital and Institute of Gerontology, Tokyo, Japan

* Correspondence: Email: kawakami-it@igakuken.or.jp

reward circuitry regions, especially in the NAcc and ventral tegmental area (VTA). Tyrosine hydroxylase (TH), calbindin, and choline O-acetyltransferase (ChAT) were utilized to identify anatomical subdivisions of the NAcc. In addition, we histochemically analyzed frozen samples, and considered the correlation between neuronal dysfunction and clinical symptoms.

Methods

Participants

Based on the reported criteria for AN,¹ we retrospectively identified five cases with binge-eating/purging-type AN in the autopsy-confirmed archives of the Department of Psychiatry; Tokyo Metropolitan Matsuzawa Hospital; the Dementia Research Project/Tokyo Metropolitan Institute of Medical Sciences; Nagoya Psychiatric Brain Bank Consortium; and the Institute for Medical Science of Aging, Aichi Medical University. Ten individuals without psychiatric or neurodegenerative disease were taken from our archives as controls (Supplementary Table S1).

Neuropathological examination

The brains were fixed in 10% formalin and embedded in paraffin. Sections 10-µm thick were cut and stained using hematoxylin-eosin, Klüver-Barrera, Holzer, and Gallyas-Braak methods. We examined alterations of the reward circuitry regions, ie, OFC, ACC, dorsal striatum, NAcc, hippocampus, mediodorsal thalamus, VTA, and substantia nigra (SN). Immunohistochemistry was performed using antibodies directed against phosphorylated tau (AT8, pSer199 and pSer202, mouse monoclonal, 1:1,000; Thermo Scientific), α-synuclein (pSyn#64, mouse monoclonal, 1:1,000; Wako), phosphorylated TDP-43 (pSer409/410, rabbit polyclonal, 1:1,000; prepared by M. Hasegawa), Aβ (E50: aa17-31, rabbit polyclonal, 1:1,000; prepared by H. Akiyama), TH (mouse monoclonal, 1:1,000; MAB318), glial fibrillary acidic protein (GFAP, rabbit polyclonal, 1:1,000, ab7260; abcam), Iba1 (polyclonal, rabbit, 1:1,000; Wako), CD68 (mouse monoclonal, 1:1,000; DAKO), calbindin D28K (polyclonal, rabbit, 1:1,000; Sigma-Aldrich), and ChAT (monoclonal,

mouse, 1:1,000; Sigma-Aldrich). Secondary immunolabeling was undertaken with a standard avidin-biotin method using an Envision Plus Kit (Dako) as previously described.¹⁴

As previously mentioned, we intensively examined the NAcc. Anatomically, the NAcc can be subdivided into inner and outer compartments (core and shell, respectively), which have distinct projections. In addition, the striatum (including NAcc) is divided into two compartments, the patch/striosome and matrix, whose neurons contain different proteins and have different afferents and efferents.¹⁵ Striosomes are associated with a subset of limbic pathways and project to the SN. In contrast, the extrastriosomal matrix is linked to sensorimotor regions and projects preferentially to the pallidothalamic and nigrostriatal pathways.¹⁶ We first aimed to identify neurochemical subdivisions of the NAcc based on immunoreactivities to TH, calbindin D28K, and ChAT antibodies. The NAcc core is consistently more intensely calbindin D28K-immunoreactive than either the medial or lateral shell in humans¹⁷ and was differentiated from the shell region. Furthermore, striosomes have low TH immunoreactivity relative to the surrounding extrastriosomal matrix and show low ChAT or calbindin immunoreactivity.^{16,18} After identification of each compartment, we investigated activated astroglial cells in each subdivision using GFAP antibody.

For double-label immunofluorescence detection, brain sections were pretreated as described above and incubated overnight at 4°C with a cocktail of appropriate primary antibodies. The sections were washed and incubated with a cocktail of Alexa568-conjugated goat anti-rabbit IgG (1:500, Vector Laboratories) and Alexa488-conjugated goat anti-mouse IgG (1:500, Vector Laboratories). After further washing, the sections were coverslipped with non-fluorescent mounting media (VECTASHIELD; Vector Laboratories) and observed with a BZ-X710 microscope (Keyence). Counts of immunopositive cells were undertaken in 7 to 9 visual fields per case that were randomly chosen from the NAcc (shell compartment) and VTA. All images were captured with the BZ-X710 microscope using the same settings. The areas of GFAP-positive cells in the NAcc were extracted and quantified by BZ-H3C Hybrid Cell Count Software (Keyence). For semiquantitative analyses of immunohistochemically stained tissue sections, the density of

Table 1. Demographic and behavioral variables for patients with AN in the present study

AN case No.	Age at onset (years)	Age at death (years)	Disease duration (years)	Sex	Body mass index (kg/m ²)*	Psychiatric symptoms				
						Depressed mood	Anxiety	Affective dysregulation	Obsessions/ compulsions	Cognitive rigidity
Case 1	14	49	25	F	10.5	+	+	+	+	+
Case 2	22	30	9	F	15.6	+	+	+		+
Case 3	20	30	10	F	na				+	+
Case 4	20	31	9	F	14.2	+				+
Case 5	11	31	20	F	9	+	+	+		+

*Terminal value retrospectively obtained from clinical records.

AN, anorexia nervosa; F, female; na, not available.

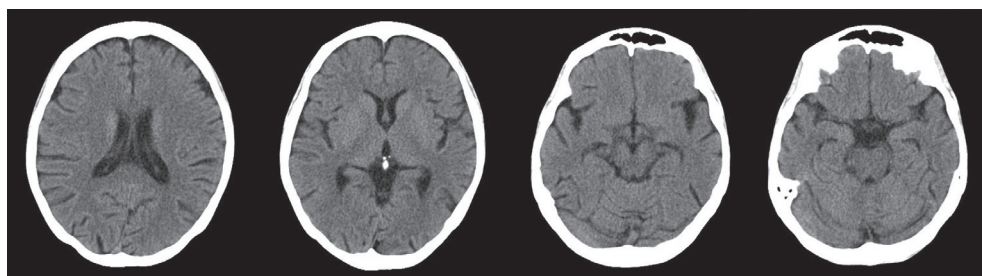


Fig.1 Computed tomography (CT) images. Selected axial CT images of an anorexia nervosa case (case #5, hospitalized, body mass index 9). These images demonstrate widespread sulcal enlargement and marked ventricular dilation.

GFAP-positive astrocytes was graded 0 for absent, ± for low, + for intermediate, ++ for high, and +++ for severe, based on microscopic observations at ×200 magnification.

The clinical and pathological findings of all cases were discussed with neuropsychiatrists and neuropathologists at clinicopathological conferences.

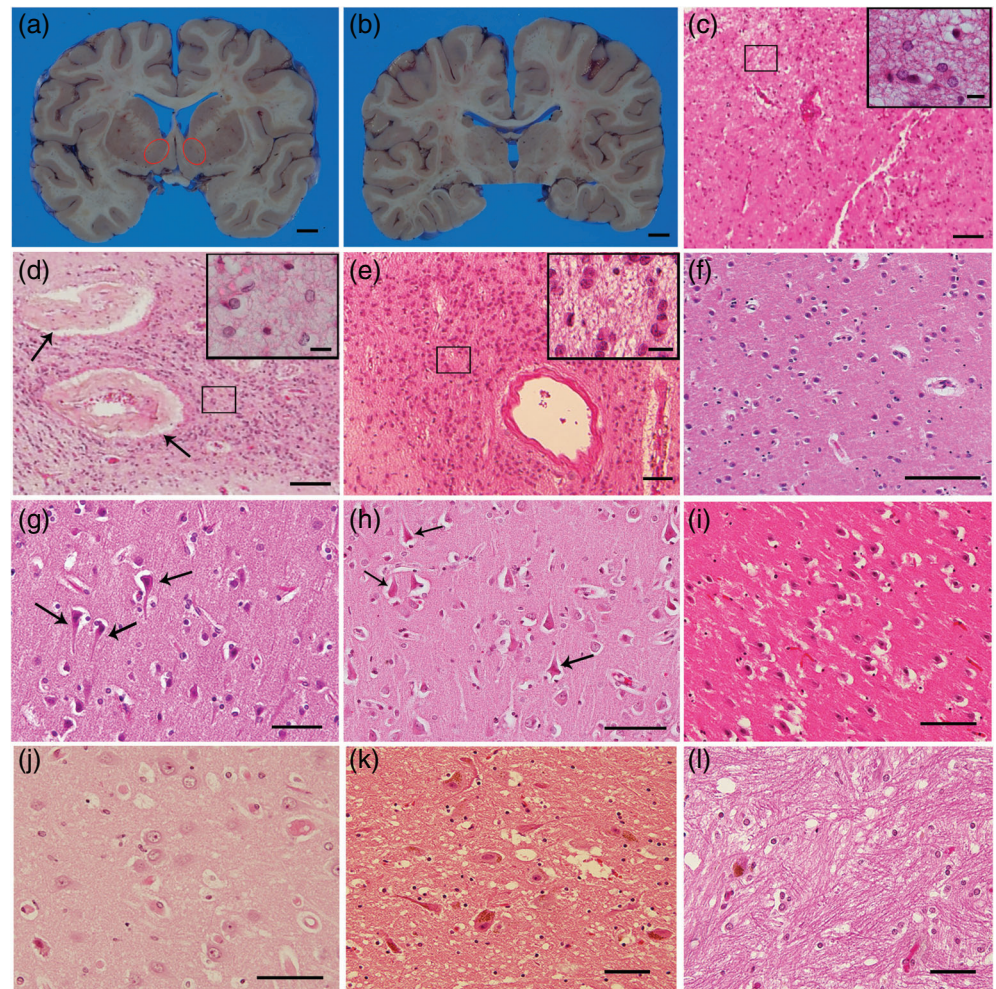


Fig.2 Neuropathologic findings of anorexia nervosa (AN) cases. Macroscopic photographs of AN case #1 (a, b). Bilateral nucleus accumbens are indicated by red circles. There is no apparent atrophy in the basal ganglia, posterior hippocampus, or neocortex. Microscopically, severe gliosis with neuronal loss in the nucleus accumbens is prominent in AN cases (c–e). The rectangle shows a high-power image of a region with fibrillary astrocytes and neuronal loss (c, case #1; d, case #2; e, case #4). The control case shows no astrogliosis or neuronal loss (f, control case). Arrows indicate ventricles with the appearance of venous collagenosis (d). The orbitofrontal cortex (g, case #2) and the anterior cingulate cortex (h, case #3) show ischemic change in neurons (marked with arrows), with a slight increase of astrocytes. Astrocytes are slightly increased in hippocampus CA1 (i, case #5) and subiculum (j, case #3). In the midbrain, some fibrillary astrocytes are seen in the SN (k, case #5) and ventral tegmental area (l, case #4). Hematoxylin–eosin staining (c–l). Scale bars, a,b: 1 cm, c: 500 μm, d–f: 100 μm (inserted figure, 10 μm), and g–l: 50 μm.

Table 2. Neuropathological data of patients with AN in the present study

AN Case (No.)	Brain weight (g)	Status of samples	Braak NFT stage/Senile plaque stage	Accumulation of α-synuclein	Accumulation of TDP-43	Increase of activated astrocytes in brain regions							
						OFC	ACC	NAcc	Striatum	Hippocampus CA1/subiculum	Mediodorsal thalamus	Midbrain	VTA
Case 1	1220	PFA	0/0	0	0	+	+	+++	+	±	+	++	+
Case 2*	1220	PFA	0/0	0	0	+	+	++	+	±	+	++	+
Case 3	1110	PFA	0/0	0	0	+	+	+	+	+	±	+	+
Case 4	1270	PFA	0/0	0	0	+	+	++	+	±	±	+	+
Case 5	1227	PFA, frozen brain	0/0	0	0	+	+	+++	+	+	+	++	++

*Ref. Umeda et al.³¹

ACC, anterior cingulate cortex; AN, anorexia nervosa; NAcc, nucleus accumbens; NFT, neurofibrillary tangle; OFC, orbitofrontal cortex; PFA, paraformaldehyde-fixed brain sections; SN, substantia nigra; TDP-43, TAR DNA-binding protein 43; VTA, ventral tegmental area.

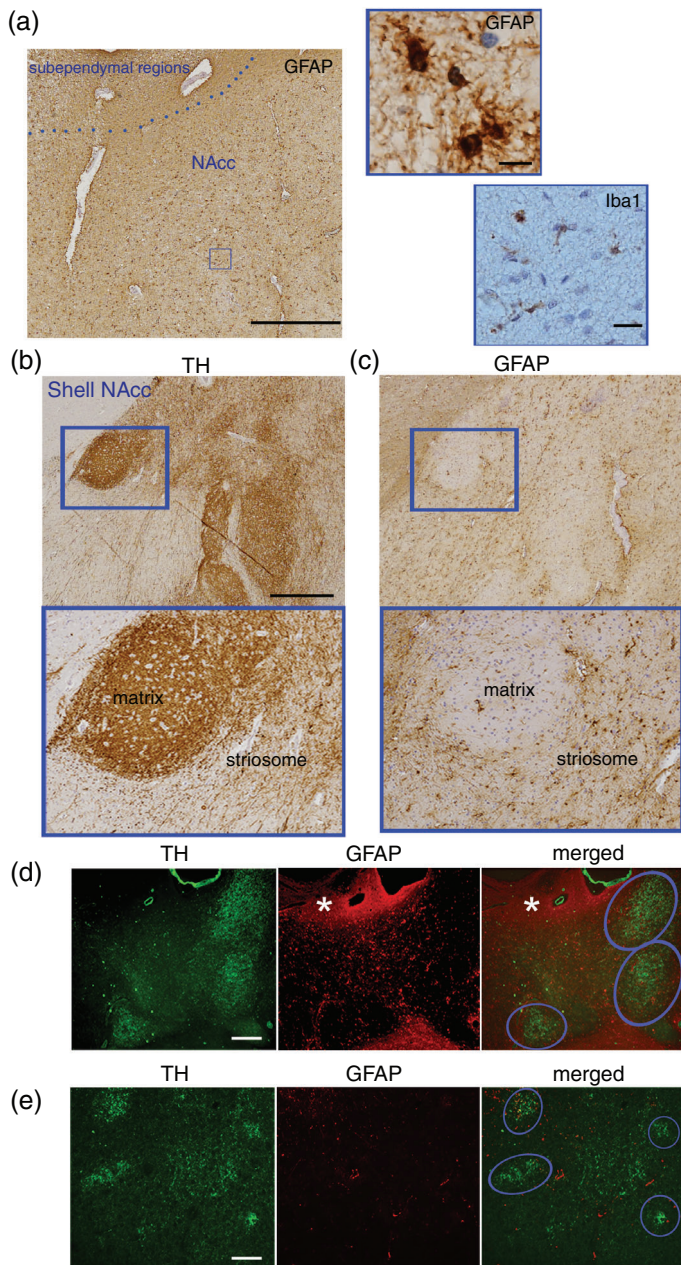


Fig.3 Immunoreactivities in the nucleus accumbens. Astroglia can be seen in the nucleus accumbens (NAcc). Moderate subependymal gliosis was present and the shell region is indicated (a, left). The rectangle shows a high-power image of a region with glial fibrillary acidic protein (GFAP)-positive astrocytes with many positive dot-like protrusions (a, right upper) and Iba1-positive activated microglial cells (a, right lower) in case #2. Serial sections in the shell (medial area) of the NAcc (b, c, case #1). Alternate sections were stained for tyrosine hydroxylase (TH; b) and GFAP (c). For B, two types of areas can be distinguished based on the modest difference in density. Patch/striosomes have a low TH immunoreactivity relative to the surrounding extrastriosomal matrix. GFAP-positive astrocytes appear preferentially in striosomes, where TH staining is relatively light. The rectangle shows a high-power image of a region with TH-positive dopaminergic neurons and GFAP-positive fibrillary astrocytes. Double immunofluorescence staining of the NAcc in AN case #1 (d) and control case #5 (e). Left: TH staining (green). Middle: GFAP staining (red). Right: merged TH and GFAP images. Blue circles indicate matrix. In AN cases, subependymal regions (white asterisks) exhibit massive GFAP-positive astrocytes. GFAP-positive astrocytes are seen preferentially in striosomes with a low intensity of TH. Control cases exhibit occasional GFAP-positive astrocyte (e). Scale bars, A: 500 μ m, (rectangle figures, 20 μ m), B: 500 μ m, and C–E: 100 μ m.

Biochemical analysis

Fresh frozen tissues (0.15–0.2 g) of the striatum and NAcc from a case with AN (one case; case #5, NAcc and dorsal striatum) and

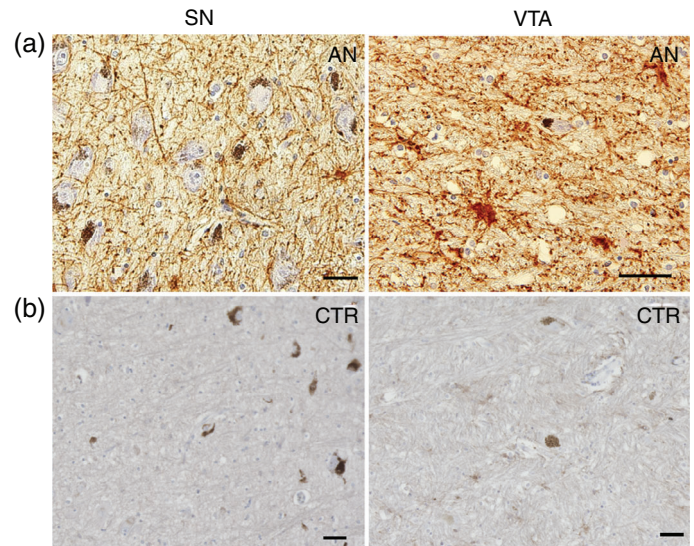


Fig.4 Immunoreactivities in midbrain. Anorexia nervosa (AN) cases show positive immunoreactivity for glial fibrillary acidic protein (GFAP) in substantia nigra (SN; a, upper) and ventral tegmental area (VTA; b, upper) without obvious neuronal loss, in comparison with the SN (a, lower) and VTA (b, lower) in control cases (CTR). Notably, the VTA in AN demonstrates GFAP-stained activated astrocytes with many positive dot-like protrusions. Case #1, CTR; case #4 (a), case #3 (b). Scale bars, a–c: 50 μ m.

controls (four cases, NAcc) were each homogenized in 10 volumes (v/v) of extraction buffer containing 50 mM Tris-HCl (pH 9.0), 1 mM EGTA, 1 mM DTT, and 0.5 mM PMSF. After centrifugation at 27 000 \times g for 10 minutes at 4°C, the supernatants were taken and the protein concentration was analyzed by BCA assay (ThermoFisher). Aliquots were mixed with 2 \times SDS sample buffer and subjected to SDS-PAGE. For immunoblotting, primary antibodies for beta actin (anti-actin, rabbit polyclonal, 1:1,000, ab8227; Abcam) and glial fibrillary acidic protein (anti-GFAP, rabbit polyclonal, 1:1,000, ab7260; Abcam) were used. Primary antibody labeling on the membranes was visualized with a Vectastain ABC kit (Vector Laboratories), using 3,3'-diaminobenzidine as a chromogen.

Statistical analysis

We compared the quantitative values of GFAP-positive astrocytes in the NAcc and VTA of AN and control cases using GraphPad Prism 7 software. The statistical significance of differences was assessed by application of the Mann-Whitney *U* test for nonparametric variables. The criterion of significant difference was set at $P < 0.05$.

Results

Demographic data

For AN cases, age at onset was 17.4 ± 4.7 years (average and standard deviation), age at death was 34.2 ± 8.3 years, disease duration was 14.6 ± 7.4 years, and terminal body mass index was 12.3 ± 3.1 . For control cases, the average age at death was 63.1 ± 11.8 years. The average brain weight of AN cases was $1,209 \pm 59.3$ g, which is within the range expected for the autopsied brain (before fixation) of an adult woman (1200–1350 g).¹⁹

The case data are summarized in Table 1. Depressed mood was seen in 80% (four cases), anxiety in 60% (three cases), affective dysregulation in 60% (three cases), obsessions/compulsions in 40% (two cases), and cognitive rigidity in 100% (five cases) of AN cases. Computed tomography scan images were obtained in one case with AN (case #5) during hospitalization, and showed widespread sulcal enlargement and marked ventricular dilation (Fig. 1).

General neuropathological findings in AN cases

There was no apparent regional atrophy in the neocortex, basal ganglia, hippocampus, midbrain, pons, or spinal cord in cases with AN (Fig. 2a,b).

Regarding neurodegenerative changes, neurofibrillary tangles (NFTs)/Aβ in the hippocampal and other regions showed Braak&Braak NFT stage 0 and Aβ stage 0 in all cases. No other aging-related proteins, including α-synuclein and TAR DNA-binding protein 43 (TDP-43), were detected (Table 2).

Increase of astrocytes in reward-related brain regions

Microscopically, severe astrogliosis with neuronal loss was prominent in the NAcc of all AN cases (Fig. 2c–e), in comparison with the NAcc in controls (Fig. 2f). Capillary blood vessels in the NAcc showed swelling of capillary endothelial cells, giving the appearance of venous collagenosis (Fig. 2d). In the striatum, moderate subependymal gliosis was present in the caudate nucleus. The OFC and ACC showed ischemic changes in neurons with a slight increase of astrocytes (Fig. 2g,h). Two cases showed a slight increase of astrocytes in hippocampus CA1 and subiculum (Fig. 2i,j). A slight increase of astrocytes was seen in the midbrain, including the SN and VTA (Fig. 2k,l). Some cases presented atrophic neurons with free melanin in the SN. There was a slight increase of astrocytes in the mediodorsal thalamus. The distribution of increased astrocytes is summarized in Table 2.

Immunoreactivity in the nucleus accumbens

Astrogliosis, which was detected with anti-GFAP immunohistochemistry, was prominent in the shell (outer) compartment of the NAcc in all of cases, although the severity varied from case to case (Fig. 3a). In addition, many positive dot-like protrusions were stained for GFAP. In the shell compartment of the NAcc, intense TH-immunostaining was observed, in accordance with previous findings.²⁰ Alternate sections of the NAcc shell were stained for TH (Fig. 3b) and GFAP (Fig. 3c), and the area showed patchy GFAP immunoreactivity. GFAP-positive astrocytes were seen preferentially in striosomes with relatively light TH staining.

Regarding activated microglial cells, there were mild increases of CD68/Iba1-positive microglial cells in both the shell and core NAcc (Fig. 3a). The distribution of microglial marker immunoreactivity in the shell compartment of the NAcc was not patchy.

TH/GFAP double immunofluorescence revealed that the astrocyte burden differed between striosome and matrix of the NAcc in all AN cases (Fig. 3d,e). AN cases displayed prominent astrogliosis in striosomes identified on the basis of low TH immunostaining (Fig. 3d). Controls showed sparse GFAP-positive astrocytes in the striosomes or matrix in the NAcc (Fig. 3e).

Immunoreactivity in midbrain

Cases with AN showed mild to moderate astrogliosis in the SN (Fig. 4a) and VTA (Fig. 4b), although neuronal loss was not obvious.

Many positive dot-like protrusions were also stained for GFAP in the midbrain of AN cases. The SN in controls presented slight astrogliosis that could have occurred as a result of normal aging.

Quantifications of GFAP-positive astrocytes

The number of GFAP-positive astrocytes in the NAcc of AN cases was significantly higher than that of controls (Mann-Whitney *U* test, *P* = 0.0079) (Fig. 5a). In the SN, there was no significant difference between AN and controls (*P* = 0.3290), whereas the number of GFAP-immunopositive astrocytes in the VTA of AN cases was significantly higher than in controls (*P* = 0.0025) (Fig. 5b).

Immunoblot analysis

Anti-actin antibody staining confirmed that approximately equal quantities of Tris-soluble fraction were applied in each case. Anti-GFAP antibody revealed 5 to 6 bands of 40 to 50 kDa corresponding to GFAP in the posterior striatum and NAcc of AN case #5 and controls. Interestingly, strongly immunoreactive bands of ≈18 to 25 kDa,

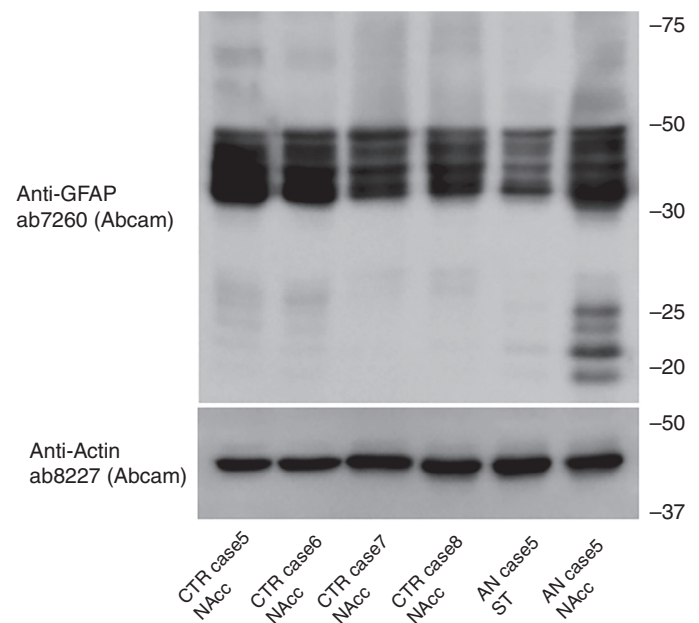
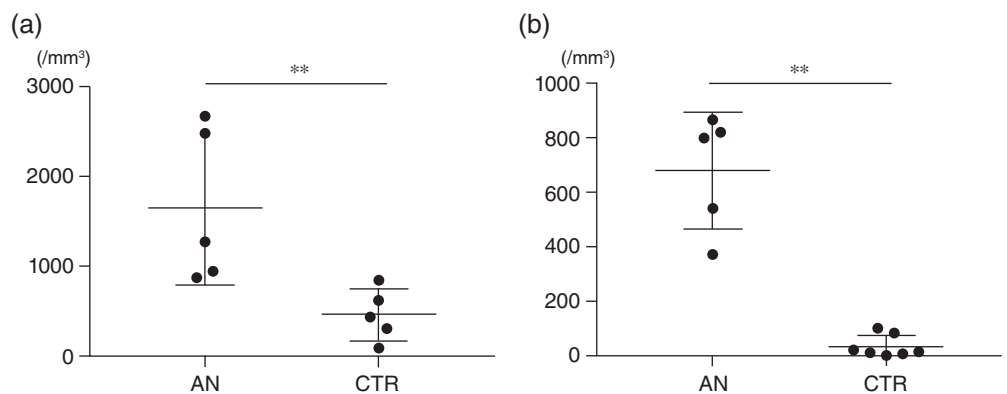


Fig.6 Biochemical analysis of anorexia nervosa (AN) cases and control cases (CTR). Sarkosyl-soluble fractions of brain tissue lysates from the posterior striatum (ST) and nucleus accumbens (NAcc) of AN case #5 and four control cases were subjected to Western blot analysis. Staining for actin (42 kDa) confirmed that approximately equal quantities were loaded. All cases show a band of 55 kDa corresponding to glial fibrillary acidic protein (GFAP) and also a GFAP-derived 48-kDa band. In AN cases, the NAcc shows strong bands at 18 to 25 kDa.

Fig.5 Quantifications of glial fibrillary acidic protein-positive astrocytes in the nucleus accumbens (NAcc) and ventral tegmental area (VTA). a, Larger amounts of positive cells (average and standard deviation are shown) were found in the NAcc of anorexia nervosa (AN) cases, compared with control cases (Mann-Whitney *U* test, ***P* = 0.0079). b, Similar results were obtained in the VTA (***P* = 0.0025).



which may represent degradation products, were detected only in the NAcc of AN cases, suggesting that abnormal GFAP degradation may occur in this region (Fig. 6).

Discussion

Dopaminergic neuronal network in AN

Anatomically, the NAcc is located in the caudal part of the anterior horn of the lateral ventricle, lying between the head of the caudate nucleus and the putamen, which forms the ventral striatum with olfactory tubercles. The NAcc can be subdivided into inner and outer parts (core and shell), and the striatum itself can be further subdivided into striosome and matrix, in addition to dorsal and ventral parts.¹⁸ The shell is considered to be more important than the core for drug-reward trigger zones and receives strong projections from the VTA.²¹ In this study, we found massive GFAP immunopositivity of astrocytes in the shell of the NAcc, with slight neuronal loss. In the medial shell, GFAP-immunopositive astrocytes were particularly distributed in the striosome portion, which is associated with a subset of limbic pathways. The VTA showed mild gliosis along the dopaminergic neurons, but without prominent neuronal loss in the region. In frontal cortex regions such as the OFC and ACC, neuronal deformation with cytoplasmic shrinkage and ischemic changes in neurons were seen, although the severity varied from case to case. VTA dopamine neurons project not only to the NAcc, but also to other limbic-related regions including the frontal cortex, hippocampus, and amygdala.²¹ In both ill and recovered AN cases, previous imaging studies have supported the notion that abnormal anatomical connectivity exists between the NAcc and frontal cortex, based on resting-state images,²² and, in addition, connectivity between the frontal cortex, insula, and NAcc has been observed in recovered AN cases.⁹

Astrocytes have a range of functions in the central nervous system.²³ In particular, astrocytic protrusions surrounding synapses, called perisynaptic astrocytic processes, are involved in synapse maturation and stability,²⁴ and correlate with the pathophysiology of depression²⁵ and schizophrenia.²⁶ In this study, AN cases showed GFAP-positive astrocytic protrusions, as well as astrocytic cells, in the NAcc and related regions. Overall, our results might indicate that NAcc pathology induces retrograde axonal degeneration in the mesolimbic pathway in AN. It seems plausible that the NAcc or VTA pathology is associated with a deficit of the reward system, although we cannot rule out an effect of hypoxic encephalopathy before death.

In this context, the presence of GFAP fragments in the NAcc might be related to disease-specific abnormalities in AN. Interestingly, similar results have been reported in other neurodegenerative diseases. Human brain immunoblots from a case of traumatic brain injury revealed a cluster of bands from 38 to 50 kDa, which were identified as GFAP and GFAP breakdown products, and the presence of GFAP autoantibodies was suggested.²⁷ Another report described the detection of proteolyzed fragments of GFAP in Western blots of autopsied striatum and SN of patients with multiple-system atrophy and progressive supranuclear palsy, together with tau-positive neurofibrillary tangles, and the authors suggested that astrogliosis might protect specific regions from damage.²⁸

In animal studies of AN, some authors have reported reduced numbers of GFAP-immunoreactive astroglial cells in the cortexes, and it has been proposed that starvation-induced neuropsychological changes may occur in patients with AN.^{29,30} However, all human postmortem studies of AN have found astrogliosis in the cortexes with neuronal degeneration.^{13,31} We consider that these astroglial changes might correlate with the severity or duration of the illness, and might be associated with a deficit of the neuronal pathways. In other words, we suggest that these changes may be a pathophysiological feature of AN.

Consequences of prolonged severe physiological stress in AN

Various mechanisms could lead to brain alterations in prolonged AN. One possibility is impaired cerebrovascular function associated with fluid shifts between the circulatory system and the interstitial space, resulting in an increased cerebrospinal fluid volume.³² Low

albumin levels have been associated with alterations in fluid shifts³³ and, indeed, most of our cases presented low albumin values. Notably, cases with idiopathic normal pressure hydrocephalus exhibit astrogliosis in the perivascular regions with enlarged ventricles,^{34,35} and the pathophysiology is reversible, as in prolonged AN. It is considered that ventricular enlargement stretches and compresses the periventricular regions, leading to interstitial edema or progressive axonal loss.^{36,37} Both disorders also exhibit demyelination of the frontal lobes and arteriolar sclerosis of the periventricular white matter,^{13,31} although the underlying mechanisms have not been clarified. Furthermore, the Wernicke encephalopathy-like pathology of some of our cases, caused by vitamin B1 deficiency, has already been described in connection with AN.^{31,38} The characteristic features of AN include gliosis, swelling of capillary endothelial cells, and capillary proliferation in the parenchymal regions. In addition, some cases showed central pontine myelinolysis, hypoxia caused by anemia, and hypoglycemia.^{31,39} Multiple factors are involved in the pathophysiology of prolonged AN, and combined approaches based on the behavioral, functional, and pathological changes of the neuroanatomical system are likely to be significant for future therapy.

Correlations between psychiatric symptoms and pathology in AN

It is well recognized that patients with AN who have a long disease duration show multiple psychiatric symptoms and are less likely to respond to psychological treatments.⁵ The cases in our study also presented various psychiatric symptoms with relatively long duration, especially cognitive rigidity, which might reflect a deficit of the reward pathway. Studies of other neurodegenerative conditions indicate that pathological changes in the pathway-related regions might induce specific psychiatric symptoms as a result of a reward circuit deficit.^{14,40} It is also possible that altered serotonin (5-hydroxytryptamine) function contributes to multiple psychiatric symptoms in AN,⁵ and serotonin–dopamine interactions might be involved. Multiple psychiatric symptoms in AN may be associated with dysregulations of various neurotransmission pathways. It would be valuable to investigate whether the neuropathological findings observed in the present study are disease-specific or are consequences of chronic malnutrition.

Limitation

We could not obtain age-matched healthy female controls in this study, as the archives in our psychiatric or neurological hospitals did not contain suitable cases. Nevertheless, our AN cases showed significantly higher levels of GFAP-immunoreactive astrocytes than the aged control cases, although it should be borne in mind that periventricular astrogliosis sometimes occurs in aged persons.

Conclusion

The cases with prolonged AN showed massive astrogliosis in the shell compartment of the NAcc and VTA. These findings may indicate that impaired functional connectivity in the reward-related network induces neuropsychiatric symptoms in AN. Structural brain abnormalities have been considered to be reversible in individuals with eating disorders, but prolonged illness might induce irreversible brain pathology. Multiple factors are certainly involved in the pathophysiology of prolonged AN. However, we consider that our results regarding the dopaminergic pathway reflect one aspect of the pathophysiology in AN, even though we cannot rule out the possibility of cachexia caused by malnutrition. Relatively new imaging modalities, such as diffusion tensor imaging, may be useful to detect axonal loss and astrogliosis for the differential diagnosis of AN. Drugs targeting dopamine receptors or astrocytic functions might be candidates for the treatment of AN in the future.⁴¹

Acknowledgments

This research was supported by The Naito Foundation (to I.K.), JSPS KAKENHI grant number 20K16660 (to I.K.), and 19K17059 (to S.I.),

AMED (JP18dm0908001 to K.O.), AMED (JP20dm0107108 to S.I.), and AMED (JP20dm0107105 to M.Y.). We thank Mr Hiroshi Gotoh, Mr Kentaro Shimizu, and Ms Kouko Ishii (Tokyo Metropolitan Matsuzawa Hospital) and Ms Hiromi Kondo and Ms Mai Kounoe (Tokyo Metropolitan Institute of Medical Science) for their excellent technical assistance.

Disclosure statement

The authors declare that they have no competing interests.

Author contributions

I.K. performed microscopy and data analysis and wrote the article. S.I., Y.R., and K.I. helped with the microscopy analysis and participated in the study design. K.N., M.Y., and K.O. organized the brain archives (including clinical information and selection of appropriate cases), and neuropathologically analyzed all cases. M.T. and M.H. contributed to sample preparation and immunoblot analysis. K.U. conceived the study and participated in its initial design. T.A. contributed to the diagnosis of general pathology and helped with the interpretation of data. M.H. participated in the study design. All authors read and approved the final article.

Ethics approval

The next of kin of all patients gave written consent for autopsy and postmortem analysis for research purposes. Adequate consideration was given to protecting case anonymity, and approval was obtained from the ethics committees of the relevant institutes for research using databases. All autopsy procedures complied with the Japanese Postmortem Examination and Corpse Preservation Act. This study was performed in accordance with the ethical standards outlined in the 1964 Declaration of Helsinki and its later amendments.

Availability of data and material

Data supporting the findings of this study are available in the supplementary material of this article. Data are also available from the corresponding author on reasonable request.

References

- American Psychiatric Association. *Diagnostic and Statistical Manual of Mental Disorders*, 5th edn. American Psychiatric Publishing, Arlington, VA, 2013.
- Strober M, Freeman R, Lampert C, Diamond J, Kaye W. Controlled family study of anorexia nervosa and bulimia nervosa: Evidence of shared liability and transmission of partial syndromes. *Am. J. Psychiatry* 2000; **157**: 393–401.
- Lipsman N, Woodside DB, Lozano AM. Neurocircuitry of limbic dysfunction in anorexia nervosa. *Cortex* 2015; **62**: 109–118.
- Attia E. Anorexia nervosa: Current status and future directions. *Annu. Rev. Med.* 2010; **61**: 425–435.
- Kaye WH, Fudge JL, Paulus M. New insights into symptoms and neurocircuit function of anorexia nervosa. *Nat. Rev. Neurosci.* 2009; **10**: 573–584.
- Garcia-Garcia I, Narberhaus A, Marques-Iturria I *et al.* Neural responses to visual food cues: Insights from functional magnetic resonance imaging. *Eur. Eat. Disord. Rev.* 2013; **21**: 89–98.
- Wang GJ, Volkow ND, Logan J *et al.* Brain dopamine and obesity. *Lancet* 2001; **357**: 354–357.
- Gervasini G, Gordillo I, Garcia-Herraiz A *et al.* Influence of dopamine polymorphisms on the risk for anorexia nervosa and associated psychopathological features. *J. Clin. Psychopharmacol.* 2013; **33**: 551–555.
- Shott ME, Pryor TL, Yang TT, Frank GK. Greater insula white matter fiber connectivity in women recovered from anorexia nervosa. *Neuropsychopharmacology* 2016; **41**: 498–507.
- DeGuzman M, Shott ME, Yang TT, Riederer J, Frank GK. Association of elevated reward prediction error response with weight gain in adolescent anorexia nervosa. *Am. J. Psychiatry* 2017; **174**: 557–565.
- Frank GK, Bailer UF, Henry SE *et al.* Increased dopamine D2/D3 receptor binding after recovery from anorexia nervosa measured by positron emission tomography and [¹¹C]raclopride. *Biol. Psychiatry* 2005; **58**: 908–912.
- Neumarker KJ, Dudeck U, Meyer U, Neumarker U, Schulz E, Schonheit B. Anorexia nervosa and sudden death in childhood: Clinical data and results obtained from quantitative neurohistological investigations of cortical neurons. *Eur. Arch. Psychiatry Clin. Neurosci.* 1997; **247**: 16–22.
- Martin F. Pathology of neurological & psychiatric aspects of various deficiency manifestations with digestive & neuro-endocrine disorders: Study of the changes of the central nervous system in 2 cases of anorexia in young girls (so-called mental anorexia). *Acta Neurol. Psychiatr. Belg.* 1958; **58**: 816–830.
- Kawakami I, Hasegawa M, Arai T *et al.* Tau accumulation in the nucleus accumbens in tangle-predominant dementia. *Acta Neuropathol. Commun.* 2014; **2**: 40.
- Gerfen CR. The neostriatal mosaic: Compartmentalization of corticostriatal input and striatonigral output systems. *Nature* 1984; **311**: 461–464.
- Graybiel AM, Moratalla R. Dopamine uptake sites in the striatum are distributed differentially in striosome and matrix compartments. *Proc. Natl. Acad. Sci. U. S. A.* 1989; **86**: 9020–9024.
- Meredith GE, Pattiselanno A, Groenewegen HJ, Haber SN. Shell and core in monkey and human nucleus accumbens identified with antibodies to calbindin-D28k. *J. Comp. Neurol.* 1996; **365**: 628–639.
- Unal B, Ibanez-Sandoval O, Shah F, Abercrombie ED, Tepper JM. Distribution of tyrosine hydroxylase-expressing interneurons with respect to anatomical organization of the neostriatum. *Front. Syst. Neurosci.* 2011; **5**: 41.
- Saukko P, Knight B. *Knight's Forensic Pathology*. CRC Press, 4th edn, London, 2015.
- Graybiel AM, Ohta K, Roffler-Tarlov S. Patterns of cell and fiber vulnerability in the mesostriatal system of the mutant mouse weaver. I. Gradients and compartments. *J. Neurosci.* 1990; **10**: 720–733.
- Ikemoto S. Brain reward circuitry beyond the mesolimbic dopamine system: A neurobiological theory. *Neurosci. Biobehav. Rev.* 2010; **35**: 129–150.
- Cha J, Ide JS, Bowman FD, Simpson HB, Posner J, Steinglass JE. Abnormal reward circuitry in anorexia nervosa: A longitudinal, multimodal MRI study. *Hum. Brain Mapp.* 2016; **37**: 3835–3846.
- Sofroniew MV, Vinters HV. Astrocytes: Biology and pathology. *Acta Neuropathol.* 2010; **119**: 7–35.
- Heller JP, Rusakov DA. Morphological plasticity of astroglia: Understanding synaptic microenvironment. *Glia* 2015; **63**: 2133–2151.
- Frizzo ME, Ohno Y. Perisynaptic astrocytes as a potential target for novel antidepressant drugs. *J. Pharmacol. Sci.* 2021; **145**: 60–68.
- Chelini G, Pantazopoulos H, Durning P, Berretta S. The tetrapartite synapse: A key concept in the pathophysiology of schizophrenia. *Eur. Psychiatry* 2018; **50**: 60–69.
- Zhang Z, Zoltewicz JS, Mondello S *et al.* Human traumatic brain injury induces autoantibody response against glial fibrillary acidic protein and its breakdown products. *PLoS One* 2014; **9**: e92698.
- Tong J, Ang LC, Williams B *et al.* Low levels of astroglial markers in Parkinson's disease: Relationship to alpha-synuclein accumulation. *Neurobiol. Dis.* 2015; **82**: 243–253.
- Frintrop L, Liesbrock J, Paulukat L *et al.* Reduced astrocyte density underlying brain volume reduction in activity-based anorexia rats. *World J. Biol. Psychiatry* 2018; **19**: 225–235.
- Frintrop L, Trinh S, Liesbrock J *et al.* The reduction of astrocytes and brain volume loss in anorexia nervosa—the impact of starvation and refeeding in a rodent model. *Transl. Psychiatry* 2019; **9**: 159.
- Umeda K, Kawakami I, Ikeda K *et al.* Case report of anorexia nervosa showing periventricular gliosis at autopsy. *Neuropathology* 2021; **41**: 127–132.
- King JA, Frank GW, Thompson PM, Ehrlich S. Structural neuroimaging of anorexia nervosa: Future directions in the quest for mechanisms underlying dynamic alterations. *Biol. Psychiatry* 2018; **83**: 224–234.
- Pirker A, Kramer L, Voller B, Loader B, Auff E, Prayer D. Type of edema in posterior reversible encephalopathy syndrome depends on serum albumin levels: An MR imaging study in 28 patients. *AJNR Am. J. Neuroradiol.* 2011; **32**: 527–531.
- Jellinger K. Neuropathological aspects of dementias resulting from abnormal blood and cerebrospinal fluid dynamics. *Acta Neurol. Belg.* 1976; **76**: 83–102.
- Tullberg M, Blennow K, Mansson JE, Fredman P, Tisell M, Wikkelso C. Ventricular cerebrospinal fluid neurofilament protein levels decrease in parallel with white matter pathology after shunt surgery in normal pressure hydrocephalus. *Eur. J. Neurol.* 2007; **14**: 248–254.
- Akai K, Uchigasaki S, Tanaka U, Komatsu A. Normal pressure hydrocephalus. Neuropathological study. *Acta Pathol. Jpn.* 1987; **37**: 97–110.

37. Siasios I, Kapsalaki EZ, Fountas KN *et al.* The role of diffusion tensor imaging and fractional anisotropy in the evaluation of patients with idiopathic normal pressure hydrocephalus: A literature review. *Neurosurg. Focus* 2016; **41**: E12.
38. Oudman E, Wijnia JW, Oey MJ, van Dam MJ, Postma A. Preventing Wernicke's encephalopathy in anorexia nervosa: A systematic review. *Psychiatry Clin. Neurosci.* 2018; **72**: 774–779.
39. Patel AS, Matthews L, Bruce-Jones W. Central pontine myelinolysis as a complication of refeeding syndrome in a patient with anorexia nervosa. *J. Neuropsychiatry Clin. Neurosci.* 2008; **20**: 371–373.
40. Patterson L, Rushton SP, Attems J, Thomas AJ, Morris CM. Degeneration of dopaminergic circuitry influences depressive symptoms in Lewy body disorders. *Brain Pathol.* 2019; **29**: 544–557.
41. Klenotich SJ, Ho EV, McMurray MS, Server CH, Dulawa SC. Dopamine D2/3 receptor antagonism reduces activity-based anorexia. *Transl. Psychiatry* 2015; **5**: e613.

Supporting information

Additional Supporting Information may be found in the online version of this article at the publisher's web-site:

Table S1. Neuropathological data of normal control cases in this study.